

Flare Occurrence in the Solar Active Regions with Reversed Helicity Sign

S. D. Bao, G. X. Ai, and H. Q. Zhang

*Beijing Astronomical Observatory/National Astronomical Observatories,
Chinese Academy of Sciences, Beijing 100012, China*

Abstract. Based on the Huairou Solar Observing Station dataset, we computed the current helicity for several hundreds of active regions and found that: (1) Active regions that do not follow the hemispheric helicity sign rule show more flare activity than normal active regions. (2) The relative number of active regions with reversed helicity sign is higher near sunspot maximum. (3) It appears that during solar cycle 22 the southern hemisphere has more the reversed-sign active regions and stronger flare activity than the northern hemisphere.

1. Introduction

Observations have revealed that a hemispheric preference of net sign of helicity, or handedness, exists throughout the solar atmosphere — in the photosphere, the chromosphere, the corona, and the solar wind (e.g., Bao, Ai, & Zhang 2000; and references therein). In the photosphere more than 70% of active regions in the northern/southern hemisphere have negative/positive current helicity (H_c or α). Zhang and Bao (1999) have found the active regions with reversed helicity sign tend to emerge at certain longitudes. Current helicity of magnetic fields also plays an important role in solar flares (Pevtsov et al. 1995, 1996; Bao et al. 1999). Canfield et al. (1999) have classified active regions according to morphology (sigmoidal or non-sigmoidal) and nature of activity (eruptive or non-eruptive), and have found that regions are significantly more likely to be eruptive if they are either sigmoidal or large. The aim of this paper is to statistically examine whether active regions with abnormal helicity sign show more flare activity.

2. Data Analysis and Results

The data we used for this study were obtained with the vector video magnetograph at the Huairou Solar Observing Station of Beijing Astronomical Observatory. The detailed description of this instrumentation and the observational technique may be found elsewhere (Wang et al. 1996; Bao et al. 2000). All vector magnetograms were observed under good weather and seeing conditions during the time when the active regions were located near the central meridian.

Bao and Zhang (1998) used the same dataset to calculate current helicity of 422 active regions in the cycle 22. They found that 84% of the active regions

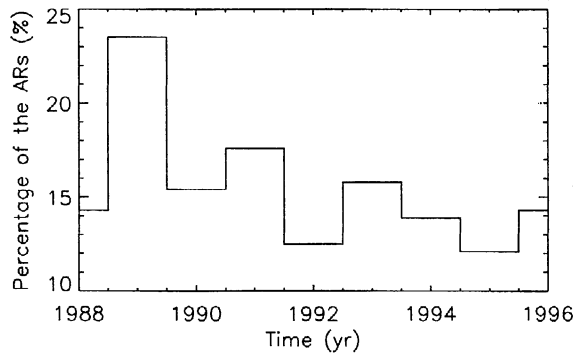


Figure 1. Distribution of the percentage of active regions that do not follow the helicity sign rule appeared on the solar disk with time.

in the northern hemisphere have negative helicity, and 79% in the southern hemisphere have positive helicity. The active regions that disobey this rule are listed in Table 1 including information on their flare activity. Most of the regions accompany by abundant flare activity. As a comparison, we also analyzed all active regions that follow the helicity sign rule, and found that active regions almost without flare activity amount to 25% of all normal active regions, but only 12% for the active regions with reversed helicity sign. In other words, these regions with reversed helicity sign have a tendency for enhanced flare activity.

Table 1 also shows that the number of active regions with reversed helicity sign reaches maximum near sunspot maximum (1989 and 1991), like other indicators of activity (such as flare count). Since the productivity of active regions is also high around sunspot maximum, we display a histogram of active regions with reversed helicity sign as a fraction of total number of active regions that appeared on the solar disk during the cycle 22 (Figure 1). This indicates that during the maximum years of solar activity the physical processes in deeper layers of the Sun are extremely complicated and dynamic, which leads to the emergence of a large number of tubes of different twisting, along with the appearance of relatively larger number of active regions with reversed helicity sign.

In addition, the north-south asymmetry can also be found in Table 1 from both the number of the reversed-sign active regions and the frequency of powerful flares occurred in these regions. Such a hemispheric asymmetry may be useful for understanding the physical conditions and processes deep below the photosphere. One should study further the relationship between flares and active regions with abnormal helicity using much larger dataset.

Acknowledgments. We are indebted to the staff of the Huairou Solar Observing Station for the observations. We also thank A.A. Pevtsov for his reading of this manuscript. This work is supported by National Science Foundation of China under grants 19791090 and 19973008.

Table 1. Synopsis of flare occurrence in the active regions with reversed helicity sign. 'l' — having some large flares exploded in an active region, 's' — only smaller flares occurred, 'm' — appearing many flares, 'f' — a few flares, and '-' — almost no flares.

NOAA/AR	Date	Coordinate	H_c	Flare class	Productivity
Northern hemisphere					
5451	19 Apr., 1989	N10 W05	+	s	m
5569	29 Jun., 1989	N21 W04	+	s	m
5589	17 Jul., 1989	N27 E04	+	s	f
5676	10 Sep., 1989	N27 W02	+	s	f
5769	04 Nov., 1989	N25 E05	+	s	m
5776	08 Nov., 1989	N17 W01	+	l	m
5796	23 Nov., 1989	N11 W05	+	-	-
5821	08 Dec., 1989	N20 E04	+	s	m
6095	10 Jun., 1990	N23 E00	+	s	m
6150	12 Jul., 1990	N07 W06	+	s	m
6199	15 Aug., 1990	N13 W04	+	s	m
6605	02 May, 1991	N09 E01	+	s	f
6792	23 Aug., 1991	N03 E01	+	-	-
6893	30 Oct., 1991	N17 E02	+	s	f
6908	10 Nov., 1991	N21 E05	+	s	f
7019	21 Jan., 1992	N17 W02	+	s	m
7029	29 Jan., 1992	N17 E01	+	-	-
7050	12 Feb., 1992	N11 W02	+	s	m
7145	27 Apr., 1992	N12 W04	+	s	f
7425	18 Feb., 1993	N15 W03	+	l	m
7448	17 Mar., 1993	N16 W04	+	l	m
7496	10 May, 1993	N15 W06	+	s	m
7512	30 May, 1993	N08 W05	+	s	f
7671	20 Feb., 1994	N11 W04	+	s	m
7794	31 Oct., 1994	N13 E05	+	s	m
7870	14 May, 1995	N10 E02	+	s	m
Southern hemisphere					
5137	19 Aug., 1988	S20 E00	-	s	f
5148	17 Sep., 1988	S11 E03	-	s	f
5212	04 Nov., 1988	S17 W06	-	s	m
5312	13 Jan., 1989	S32 E04	-	l	m
5497	23 May, 1989	S20 E01	-	l	m
5622	05 Aug., 1989	S27 E01	-	l	m
5657	23 Aug., 1989	S20 E08	-	-	-
5669	05 Sep., 1989	S17 E01	-	l	m
5747	20 Oct., 1989	S26 W01	-	l	m
5801	26 Nov., 1989	S20 E00	-	-	-
5947	26 Feb., 1990	S17 W04	-	s	m
6050	09 May, 1990	S11 E03	-	s	f
6064	19 May, 1990	S15 W01	-	l	m
6131	03 Jul., 1990	S21 W02	-	l	m
6227	26 Aug., 1990	S23 W02	-	l	m
6462	27 Jan., 1991	S18 E06	-	s	m
6509	24 Feb., 1991	S21 E03	-	s	f
6593	21 Apr., 1991	S12 W06	-	l	m
6615	06 May, 1991	S11 W04	-	s	m
6698	30 Jun., 1991	S05 W04	-	-	-
6818	04 sep., 1991	S12 W02	-	l	m
6873	15 Oct., 1991	S23 W07	-	s	m
7026	27 Jan., 1992	S13 E00	-	s	f
7039	04 Feb., 1992	S15 W03	-	l	m

Table 1. — *Continued*

NOAA/AR	Date	Coordinate	H_c	Flare class	Productivity
7335	12 Nov., 1992	S18 W06	—	s	f
7345	23 Nov., 1992	S24 W04	—	l	m
7400	13 Jan., 1993	S09 W04	—	s	m
7411	26 Jan., 1993	S12 E01	—	s	m
7493	04 May., 1993	S10 W03	—	s	f
7563	17 Aug., 1993	S04 W04	—	s	m
7625	30 Nov., 1993	S15 W01	—	-	-
7629	08 Dec., 1993	S21 E00	—	s	m
7742	03 Jul., 1994	S09 E00	—	s	f
7792	24 Oct., 1994	S08 E04	—	s	f
7815	14 Dec., 1994	S11 W05	—	l	m
7842	20 Feb., 1995	S14 E06	—	-	-
7854	21 Mar., 1995	S17 W02	—	s	m
7921	12 Nov., 1995	S10 E01	—	s	f
7999	26 Nov., 1996	S05 E05	—	s	m

References

- Bao, S. D., Ai, G. X., & Zhang, H. Q. 2000, *J. Astrophys. Astr.*, in press
- Bao, S. D., Pevtsov, A. A., Wang, T. J., & Zhang, H. Q. 2000, *Solar Phys.*, 195, 75
- Bao, S. D. & Zhang, H. Q. 1998, *ApJ*, 496, L43
- Bao, S. D., Zhang, H. Q., Ai, G. X., & Zhang, M. 1999, *A&AS*, 139, 311
- Canfield, R. C., Hudson, H. S., & McKenzie, D. E. 1999, *Geophysical Research Letters*, 26, 627
- Pevtsov, A. A., Canfield, R. C., & Metcalf, T. R. 1995, *ApJ*, 440, L109
- Pevtsov, A. A., Canfield, R. C., & Zirin, H. 1996, *ApJ*, 473, 533
- Zhang, H. Q. & Bao, S. D. 1999, *ApJ*, 519, 876
- Wang J. X., Shi Z. X., Wang H. N., & Lü Y. P. 1996, *ApJ*, 456, 861